Chapter 7

Constraint Handling Optimal PI Controller Design for Integrating Processes: Optimization-Based Approach for Analytical Design

Rodrigue Tchamna and Moonyong Lee

Additional information is available at the end of the chapter

http://dx.doi.org/10.5772/intechopen.74301

Abstract

This chapter introduces the closed-form analytical design of proportional-integral (PI) controller parameters for the optimal control subjected to operational constraints. The main idea of the design is not only to minimize the control performance index but also to cope with the constraints in the process variable, controller output, and its rate of change. The proposed optimization-based approach is examined to regulatory and servo control of integrating processes with three typical operation constraints. To derive an analytical design formula, the constrained optimal control problem in the time domain was transformed to an unconstrained optimization in a new parameter space associated with closed-loop dynamics. By taking the advantage of the proposed analytical approach, the optimal PI parameters can be found quickly based on the graphical analysis without complex numerical optimization. The resulting optimal PI controller guarantees the globally optimal closed-loop response and handles the operational constraints precisely.

Keywords: constrained optimal control, industrial PI controller, analytical design, constraint handling, integrating process, optimal servo and regulatory control

1. Introduction

Many units used in the chemical process industry, such as heating boilers, batch chemical reactors, liquid storage tanks, or liquid level systems, are integrating processes in which the dynamic response is very slow with a large dominant time constant. In modern control, the integrating process also appears in many applications including space telescope control systems, lightweight robotic arms, and pilot crane control systems. Constraints are inherent in

any industrial control systems, either implicitly or explicitly. They are generally associated with both the process variable and controller output. Indeed, typical operational constraints usually include the actuator magnitude and its rate saturation, process/output variable, and internal state variables. The objective of constrained optimal control is to minimize the control cost subjected to constraints on state variables and/or output variables. The importance of taking constraints into account during the design stage of the controller is no more questioned. In fact, a well-designed optimal control would fail in a real-life situation if the constraints are not taken into account while designing the controller. However, optimal control of a process with multiple constraints is still challenging even for a process with simple dynamics. In a popular approach using Pontryagin's principle or the Hamilton-Jacobi-Bellman equation for a classical optimal control framework [1, 2], the optimal controller parameters are obtained via numerical solution of the nonlinear constrained optimization. However, the existing numerical methods neither guarantee a global optimal solution nor provide useful insights and physical interpretations of the complex relationships existing between the process parameters and control performance. To address this issue, the analytical solutions of optimal proportional-integral (PI) controller under constraints were previously proposed using the optimization-based approach for integrating systems [3–7] and extended to first-order systems [8–11]. This chapter introduces the optimization-based approach for the analytical design of optimal PI controller parameters for integrating processes without violating the operational constraints under a unified framework.

2. Formulation of constrained optimal PI control problem

Figure 1 presents the schematic diagram of an integrating process considered in this chapter. It is a type-C PI controller, also called I-P controller, which is a modified type of PID controller where the set point is removed from the proportional term in order to avoid the initial quick on the manipulated variable for a step change in the set point.

The major resulting transfer functions of this closed-loop system are expressed as

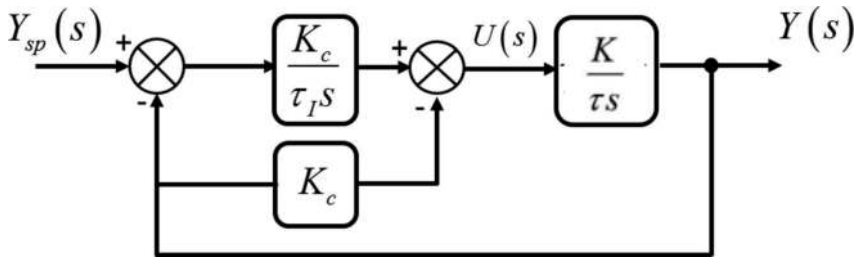

Figure 1. Block diagram of the feedback control of integrating process.

$$Y(s) = \frac{1}{\tau_c \tau_1 s^2 + \tau_I s + 1} Y_{sp}(s) + \frac{K_p \tau_c \tau_I s}{\tau_c \tau_I s^2 + \tau_I s + 1} D(s) \tag{1}$$

$$U(s) = \frac{1}{K_p} \frac{s}{\tau_c \tau_1 s^2 + \tau_I s + 1} Y_{sp}(s) - \frac{\tau_I s + 1}{\tau_c \tau_I s^2 + \tau_I s + 1} D(s) \tag{2}$$

where

$$\tau_c = \frac{1}{K_p K_c};\ K_p = \frac{K}{\tau} \tag{3}$$

The closed-loop damping ratio of the above system becomes

$$\zeta = \frac{1}{2}\sqrt{\frac{\tau_I}{\tau_c}} \tag{4}$$

The goal of a constrained optimal problem is to minimize the weighted sum of the process variable error, e(t), and the rate of change in the manipulated variable, u′(t), for a given step change, $\Delta D/s$, in disturbance (i.e., optimal regulatory control) or that, $\Delta Y_{sp}/s$, in set point (i.e., optimal servo control) subjected to the following three typical operational constraints: the maximum allowable limit in (1) the controlled variable, $y_{\max}$, (2) the rate of change in the manipulated variable, $u'_{\max}$, and (3) the manipulated variable, $u_{\max}$.

Consequently, the constrained optimal control problem is formulated as

$$\min \Phi = \int_0^\infty \left[\omega_y \left(y(t) - y_{sp}(t) \right)^2 + \omega_{u'} (u'(t))^2 \right] dt \tag{5a}$$

subject to

$$|y(t)| \le y_{\max} \tag{5b}$$

$$|u'(t)| \le u'_{\max} \tag{5c}$$

$$|u(t)| \le u_{\max} \tag{5d}$$

Through some mathematical operations, the above optimal control problem formulated in the time domain can be transformed to the form with the two new design parameters ζ and τ_c as expressed in **Table 1**. As shown in **Table 1**, the three constraints are also expressed as only a function of ζ and τ_c. Then, a simple graphical examination of the contour of the objective function and the constraints in (ζ, τ_c) space allows to find the location of global optimal solution without complex numerical optimization process.

	Regulatory control	**Servo control**
Objective function	$\min\Phi_r(\zeta,\tau_c)=\alpha\tau_c^3\zeta^2+\frac{\beta}{\tau_c}\left(\frac{1}{4\zeta^2}+1\right)$	$\min\Phi_s(\zeta,\tau_c)=\alpha\tau_c\left(4\zeta^2+1\right)+\frac{\beta}{\tau_c^3\zeta^4}$
Constraints	$\tau_c g_r(\zeta)\le\gamma_g$ $h_r(\zeta,\tau_c)\le\gamma_h$ $f_r(\zeta,\tau_c)\le\gamma_f$	$g_s(\zeta)\le\gamma_g$ $h_s(\zeta)\le\tau_c^2\gamma_h$ $f_s(\zeta,\tau_c)\le\gamma_f$
Parameters	$\alpha=2\omega_y\left(K_p\Delta D\right)^2;\beta=\frac{\omega_{u'}}{2}(\Delta D)^2;$ $\gamma_g=\left\lvert\frac{y_{\max}}{K_p\Delta D}\right\rvert;\gamma_h=\left\lvert\frac{u'_{\max}}{\Delta D}\right\rvert;\gamma_f=\left\lvert\frac{u_{\max}}{\Delta D}\right\rvert$	$\alpha=\frac{\omega_y\Delta Y_{sp}^2}{2};\ \beta=\frac{\omega_{u'}}{32}\left(\frac{\Delta Y_{sp}}{K_p}\right)^2;$ $\gamma_g=\left\lvert\frac{y_{\max}}{\Delta Y_{sp}}\right\rvert;\gamma_h=\left\lvert\frac{K_p u'_{\max}}{\Delta Y_{sp}}\right\rvert;\gamma_f=\left\lvert\frac{K_p\tau_c u_{\max}}{\Delta Y_{sp}}\right\rvert$
Functions g,h,f	$g_r(\zeta)=\frac{2}{\sqrt{1+x^2}}\exp\left(-\frac{\tan^{-1}x}{x}\right)$ for $0<\zeta<1$ $=2\exp(-1)$ for $\zeta=1$ $=\frac{2}{\sqrt{1-x^2}}\exp\left(-\frac{\tanh^{-1}x}{x}\right)$ for $\zeta>1$	$g_s(\zeta)=1+\exp\left(-\frac{\pi}{x}\right)$ for $0<\zeta<1$ $=1$ for $\zeta\ge1$ where $x=\frac{\sqrt{1-\zeta^2}}{\zeta}$ for $0<\zeta\le1$ $=\frac{\sqrt{\zeta^2-1}}{\zeta}$ for $\zeta>1$
	$h_r(\zeta,\tau_c)=\frac{1}{2\tau_c\zeta}\exp\left[-\frac{1}{x}\tan^{-1}\left(\frac{4\zeta^2-1}{4\zeta^2-3}x\right)\right]$ for $\zeta<\frac{1}{2}$ $=\left\lvert\frac{u'(0)}{\Delta D}\right\rvert=\frac{1}{\tau_c}$ for $\zeta\ge\frac{1}{2}$	$h_s(\zeta)=\frac{1}{4\zeta^2}$ for $\zeta>0$
	$f_r(\zeta,\tau_c)=1+\exp\left\{-\frac{1}{x}\tan^{-1}\left[\frac{2\zeta^2}{2\zeta^2-1}x\right]-\frac{\pi}{x}\right\}$ for $0<\zeta<\frac{1}{\sqrt{2}}$ $=1+\exp\left\{-\frac{1}{x}\tan^{-1}\left[\frac{2\zeta^2}{2\zeta^2-1}x\right]\right\}$ for $\frac{1}{\sqrt{2}}\le\zeta<1$ $=1+\exp(-2)$ for $\zeta=1$ $=1+\exp\left\{-\frac{1}{x}\tanh^{-1}\left[\frac{2\zeta^2}{2\zeta^2-1}x\right]\right\}$ for $\zeta>1$	$f_s(\zeta,\tau_c)=\frac{1}{2\zeta}\exp\left(-\frac{1}{x}\tan^{-1}x\right)$ for $0<\zeta<1$ $=\frac{1}{2}\exp(-1)$ for $\zeta=1$ $=\frac{1}{2\zeta}\exp\left(-\frac{1}{x}\tanh^{-1}x\right)$ for $\zeta>1$

Table 1. Objective function and constraints of the optimal control problem in (ζ,τ_c) space.

3. PI controller design

3.1. Optimal regulatory control

Applying the Lagrangian multiplier [12], it converts the constrained optimization problem in **Table 1** to an equivalent unconstrained problem. In regulatory control, the constrained problem can be converted as

$$\begin{aligned}\min \mathrm{L}(\zeta, \tau_{\mathrm{c}}, \varpi, \sigma) = \Phi_r(\zeta, \tau_{\mathrm{c}}) + \varpi_1\left(\gamma_{\mathrm{h}} - h_r(\zeta, \tau_{\mathrm{c}}) - \sigma_1^2\right) \\ + \varpi_2\left(\gamma_{\mathrm{g}} - g_r(\zeta)\tau_c - \sigma_2^2\right) + \varpi_3\left(\gamma_{\mathrm{f}} - f_r(\zeta, \tau_{\mathrm{c}}) - \sigma_3^2\right)\end{aligned} \tag{6}$$

where ϖ_i and σ_i are the Lagrange multiplier and the slack variable, respectively.

The necessary conditions for an optimal solution are then

$$\frac{\partial L}{\partial \tau_{\mathrm{c}}} = \frac{\partial \Phi_r}{\partial \tau_{\mathrm{c}}} + \varpi_1\left[-\frac{\partial h_r(\zeta, \tau_{\mathrm{c}})}{\partial \tau_{\mathrm{c}}}\right] + \varpi_2\left[-g_r(\zeta)\right] + \varpi_3\left[-\frac{\partial f_r(\zeta, \tau_{\mathrm{c}})}{\partial \tau_{\mathrm{c}}}\right] = 0 \tag{7a}$$

$$\frac{\partial L}{\partial \zeta} = \frac{\partial \Phi_r}{\partial \zeta} - \varpi_1 \frac{\partial h_r(\zeta, \tau_{\mathrm{c}})}{\partial \zeta} - \varpi_2 \tau_c \frac{\partial g_r(\zeta)}{\partial \zeta} - \varpi_3 \frac{\partial f_r(\zeta, \tau_{\mathrm{c}})}{\partial \zeta} = 0 \tag{7b}$$

$$\frac{\partial L}{\partial \varpi_1} = \gamma_{\mathrm{h}} - h_r(\zeta, \tau_{\mathrm{c}}) - \sigma_1^2 = 0;\ \frac{\partial L}{\partial \varpi_2} = \gamma_g - \tau_{\mathrm{c}} g_r(\zeta) - \sigma_2^2 = 0;\ \frac{\partial L}{\partial \varpi_3} = \gamma_{\mathrm{f}} - f_r(\zeta, \tau_c) - \sigma_3^2 = 0 \tag{7c}$$

$$\frac{\partial L}{\partial \sigma_1} = -2\varpi_1\sigma_1 = 0;\ \frac{\partial L}{\partial \sigma_2} = -2\varpi_2\sigma_2 = 0;\ \frac{\partial L}{\partial \sigma_3} = -2\varpi_3\sigma_3 = 0 \tag{7d}$$

The simultaneous solutions of Eqs. (7a)–(7d) for possible combinations of $\sigma_i = 0$, $\sigma_i \neq 0$, $\varpi_i = 0$, and $\varpi_i \neq 0$ are associated with the corresponding optimal cases. Note that instead of introducing the slack variables, Karush-Kuhn-Tucker conditions [13] can also be utilized for solving the constrained optimization problem, which finds the same optimal PI parameters by the Lagrangian multiplier method.

Figure 2 presents seven possible cases for the location of global optima: the global optimum can be found inside the feasible region (case A), or on the boundary of one constraint (cases B, C, and E), or on the intersection point of two constraints (cases D, F, and G).

The global optima of the seven cases can be evaluated by inspecting their geometrical characteristics in (ζ, τ_c) space as well as the corresponding conditions of the Lagrange multipliers and slack variables as follows:

Case A $(\varpi_1 = \varpi_2 = \varpi_3 = 0)$: The extreme point, $\left(\zeta^{\dagger}, \tau_c^{\dagger}\right)$, which is located inside the feasible region, is therefore the global optimum. Solving Eqs. (7a) and (7b) simultaneously, the global optimum can be determined in explicit form as

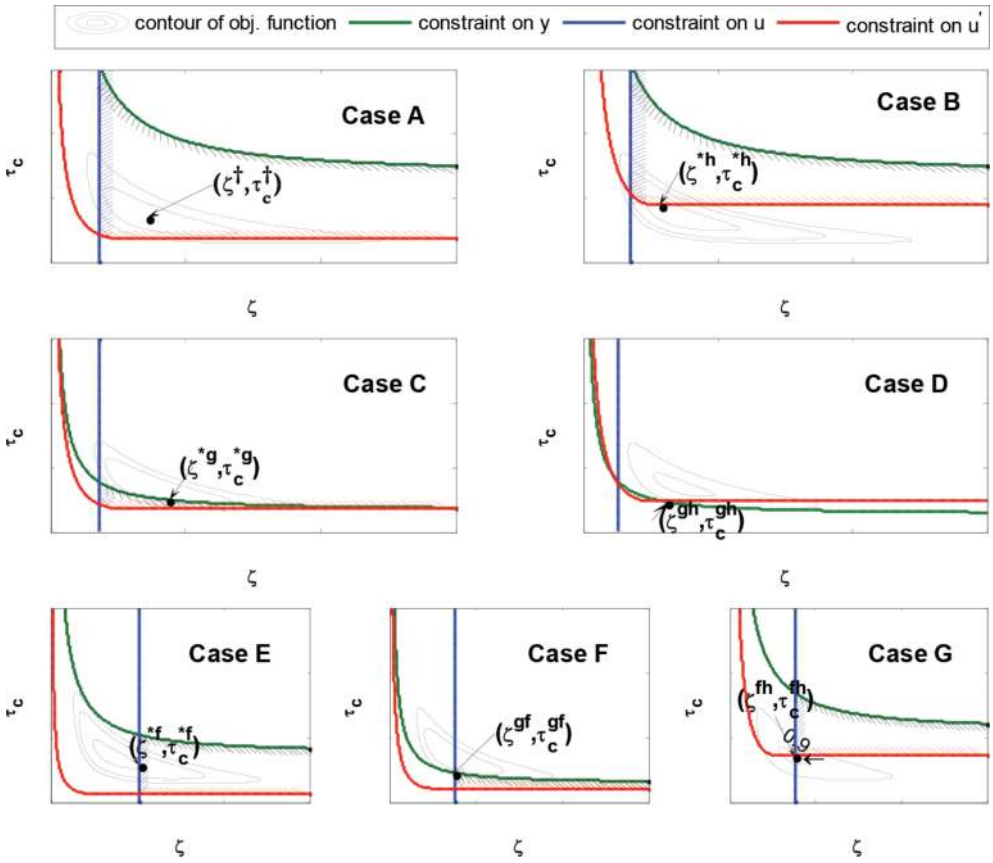

Figure 2. Contours, constraints, and possible locations of the global optimum in regulatory control case.

$$\zeta^{\dagger} = \sqrt{\frac{1}{2}} \tag{8a}$$

$$\tau_c^{\dagger} = \left(\frac{\beta}{\alpha}\right)^{1/4} \tag{8b}$$

Case B ($\sigma_1 = \varpi_2 = \varpi_3 = 0$): The global optimum, symbolized as $\left(\zeta^{*\mathrm{h}}, \tau_{\mathrm{c}}^{*\mathrm{h}}\right)$, is positioned on the constraint, $\gamma_{\mathrm{h}} = h_r(\zeta, \tau_{\mathrm{c}})$. $\zeta^{*\mathrm{h}}$ and $\tau_{\mathrm{c}}^{*\mathrm{h}}$ can be obtained by substituting $\sigma_1 = \varpi_2 = \varpi_3 = 0$ into the equation of necessary conditions, thus solving the following system of equations:

$$\gamma_{\mathrm{h}} - h_r(\zeta, \tau_c) = 0 \tag{9a}$$

$$\frac{\partial \Phi_r}{\partial \zeta} - \frac{\partial \Phi_r}{\partial \tau_c}\left[\frac{\partial h_r}{\partial \tau_c}\right]^{-1}\frac{\partial h_r}{\partial \zeta} = 0 \tag{9b}$$

Case C ($\varpi_1 = \sigma_2 = \varpi_3 = 0$): The global optimum, $\left(\zeta^{*g}, \tau_c^{*g}\right)$, is located on the constraint, $\gamma_g = \tau_c g_r(\zeta)$, and obtained by solving the following system of equations:

$$\gamma_g - g_r(\zeta)\tau_c = 0 \tag{10a}$$

$$\frac{\partial \Phi_r}{\partial \zeta} g_r - \tau_c \frac{\partial \Phi_r}{\partial \tau_c} \frac{\partial g_r}{\partial \zeta} = 0 \tag{10b}$$

Case D ($\sigma_1 = \sigma_2 = \varpi_3 = 0$): The global optimum represented by $\left(\zeta^{gh}, \tau_c^{gh}\right)$ is located on the intersection point by $\gamma_h = h_r(\zeta, \tau_c)$ and $\gamma_g = \tau_c g_r(\zeta)$, thus can be calculated by solving

$$\gamma_g - \tau_c g_r(\zeta) = 0 \tag{11a}$$

$$\gamma_h - h_r(\zeta, \tau_c) = 0 \tag{11b}$$

Case E ($\varpi_1 = \varpi_2 = \sigma_3 = 0$): The global optimum, $\left(\zeta^{*f}, \tau_c^{*f}\right)$, is located on the constraint, $\gamma_f = f_r(\zeta, \tau_c)$, and can be found by solving

$$\gamma_f - f_r(\zeta, \tau_c) = 0 \tag{12a}$$

$$\frac{\partial f_r}{\partial \tau_c} \frac{\partial \Phi_r}{\partial \zeta} - \frac{\partial f_r}{\partial \zeta} \frac{\partial \Phi_r}{\partial \tau_c} = 0 \tag{12b}$$

Case F ($\varpi_1 = \sigma_2 = \sigma_3 = 0$): The global optimum, $\left(\zeta^{gf}, \tau_c^{gf}\right)$, which is on the intersection point created by $\gamma_f = f_r(\zeta, \tau_c)$ and $\gamma_g = \tau_c g_r(\zeta)$, is calculated by solving

$$\gamma_f - f_r(\zeta, \tau_c) = 0 \tag{13a}$$

$$\gamma_g - \tau_c g_r(\zeta) = 0 \tag{13b}$$

Case G ($\sigma_1 = \varpi_2 = \sigma_3 = 0$): The global optimum, $\left(\zeta^{fh}, \tau_c^{fh}\right)$, is located on the intersection point of the constraints $\gamma_f = f_r(\zeta, \tau_c)$ and $\gamma_h = h_r(\zeta, \tau_c)$, and calculated by solving

$$\gamma_f - f_r(\zeta, \tau_c) = 0 \tag{14a}$$

$$\gamma_h - h_r(\zeta, \tau_c) = 0 \tag{14b}$$

After the global optimum is determined in (ζ, τ_c) space, the optimal PI parameters corresponding to each case can then be calculated from Eqs. (3) and (4) as

$$K_c^{opt} = \frac{1}{K_p \tau_c^{opt}}; \tau_I^{opt} = 4\left(\zeta^{opt}\right)^2 \tau_c^{opt} \tag{15}$$

One of main advantages of the optimization-based graphical approach is that the conditions for the seven possible cases can be directly evaluated based on a meticulous analysis of the

graphical shape of the constraints and contours in (ζ, τ_c) space. The concept of the relative locations between the extreme point and its projections to the constraints is used mainly to develop the conditions to discriminate each case associated with the corresponding global optimum. **Figure 3** shows an example of the projection of the extreme point and its notation rule used in this graphical analysis for the optimal PI design. The notation, $\zeta^{\dagger f}$, represents the abscissa of the projection of the extreme point on the constraint curve by *f*. Similarly, $\tau_c^{\dagger h}$ and $\tau_c^{\dagger g}$ indicate the ordinate of the projection of the extreme point on the constraint curves by *h* and *g*, respectively. If $\tau_c^{\dagger}$ is such that $\tau_c^{\dagger h} \le \tau_c^{\dagger} \le \tau_c^{\dagger g}$, then the global optimum is above the constraint, *h*, and below the constraint, *g*. Referring to **Figure 2**, this corresponds to cases A, E, or possibly G. In this case, it is apparent from **Figure 2** that if $\zeta^{\dagger f} < \zeta^{\dagger}$, it belongs to case A (i.e., the extreme point is the global optimum), otherwise it belongs to either case E or G. Cases E and G can be distinguished simply by comparing τ_c^{*f} and τ_c^{fh}, where τ_c^{fh} is the ordinate of the intersection of the constraints by *f* and *h*. As seen in **Figure 2**, if $\tau_c^{*f} > \tau_c^{fh}$, the global optimum case belongs to case E, otherwise case G.

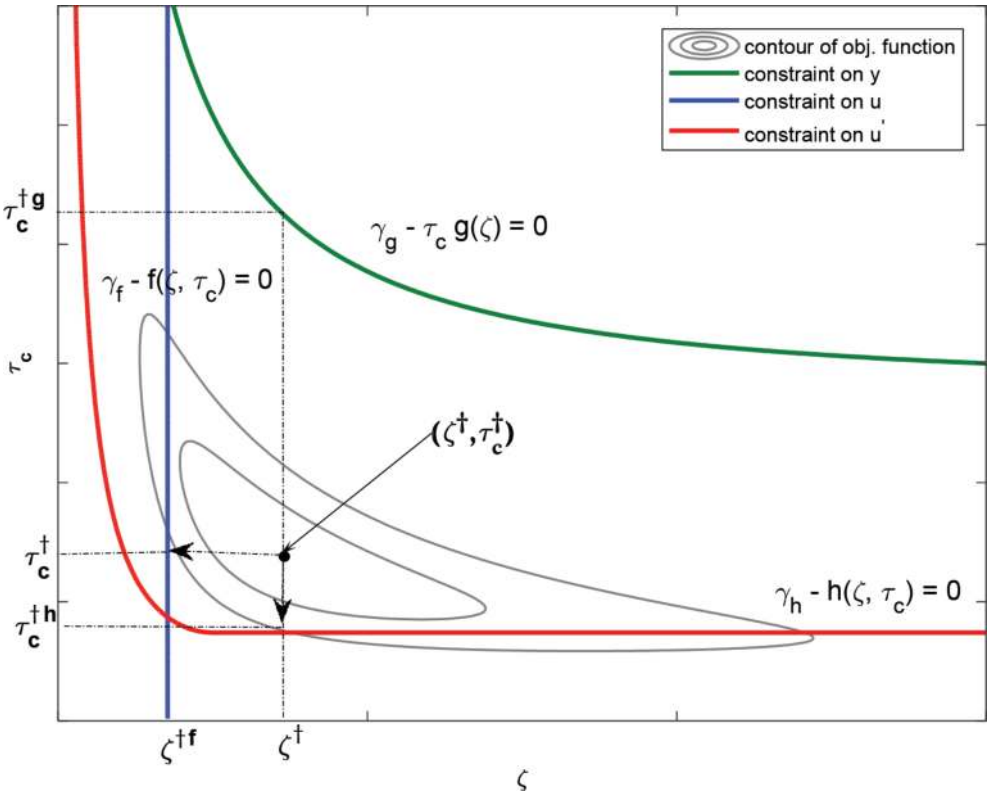

Figure 3. Projection of the extreme point on the constraints in (ζ, τ_c) space.

Using similar reasoning, the conditions to discriminate each of seven cases associated with the global optimum can be established according to the relative locations between the extreme point and its projections to the constraints. **Table 2** lists the results for the conditions and characteristics of the global optima.

3.2. Optimal servo control

The constrained optimization problem in **Table 1** can be converted into an equivalent unconstrained problem by applying the Lagrangian multiplier [12] as follows:

$$\begin{aligned}\min L(\tau_c, \zeta, \varpi, \sigma) = \alpha\tau_c\left(4\zeta^2+1\right) + \frac{\beta\left(4\tau_c^2\zeta^2+\tau^2\right)}{\tau^2\tau_c^3\zeta^4} + \varpi_1\left(\tau_c^2\gamma_h - h_s(\zeta) - \sigma_1^2\right) \\ + \varpi_2\left(\gamma_g - g_s(\zeta) - \sigma_2^2\right) + \varpi_3\left(\gamma_f - f_s(\zeta,\tau_c) - \sigma_3^2\right)\end{aligned} \tag{16}$$

where ϖ_i and σ_i are the Lagrange multiplier and the slack variable, respectively.

Applying the same way used in the regulatory control case, the seven optimal cases can be found by solving the necessary conditions of the above unconstrained problem for the corresponding combination of slack variable and Lagrange multiplier. **Figure 4** illustrates the seven possible locations of the global optimum.

After obtaining the global optimum for a particular case, the optimal parameters of the PI controller can be calculated using Eq. (15), i.e., $K_c = 1/K_p\tau_c^{opt}; \tau_I = 4\left(\zeta^{opt}\right)^2\tau_c^{opt}$. **Table 3** summarizes the conditions that lead to each global optimal location.

4. Design and evaluation of feasible constraints

The optimal solutions in **Tables 2** and **3** are only true if the constraint set is such that a solution exists. Indeed, depending on the constraint set, the optimal solution may not have a feasible solution. Therefore, before applying the constrained optimal control formulation, either any given constraint set should first be screened quickly to determine its basic feasibility or a constraint set should be designed to be feasible.

4.1. Optimal regulatory control

Conditions for a feasible $\left(y_{max}, u'_{max}\right)$: For a given y_{max}, there is a minimum available u'_{max} value below which the optimal control problem is not feasible. **Figure 5** demonstrates the effects of the constraint specifications on the feasible region in (ζ, τ_c) space. The constraint imposed by Eq. (5d) lies on a vertical line that shifts and bends rightward as u_{max} decreases. The constraint given in Eq. (5c) shifts upward as u'_{max} decreases, whereas the constraint in Eq. (5b) shifts downward as y_{max} decreases. Note that the feasible region only exists when the constraint curve of u'_{max} is below that of y_{max}.

Case	Constraint specification	Condition	Global optimum	Location of global optimum	Calculation of global optimum
A	Mild $y_{\max}$ Mild $u'_{\max}$ Mild $u_{\max}$	$\left[\zeta^{\dagger f} \le \zeta^{\dagger}\right] \cap \left[\tau_c^{\dagger h} \le \tau_c^{\dagger} \le \frac{\gamma_g}{g_r(\zeta^{\dagger})}\right]$	$(\zeta^{\dagger}, \tau_c^{\dagger})$	In the interior of the feasible region	$\zeta^{\dagger} = \sqrt{\frac{1}{2}}$ $\tau_c^{\dagger} = \left(\frac{\beta}{\alpha}\right)^{1/4}$
B	Mild $y_{\max}$ Tight $u'_{\max}$ Mild $u_{\max}$	$\left[\zeta^{\dagger f} \le \zeta^{*h} \le \zeta^{gh}\right] \cap \left[\tau_c^{\dagger} < \tau_c^{\dagger} h\right]$	$(\zeta^{*h}, \tau_c^{*h})$	On $\gamma_h = h_r(\zeta, \tau_c)$	$\gamma_{\mathrm{h}} - h_r(\zeta, \tau_c) = 0$ $\frac{\partial \Phi_r}{\partial \zeta} - \frac{\partial \Phi_r}{\partial \tau_c}\left[\frac{\partial h_r}{\partial \tau_c}\right]^{-1} \frac{\partial h_r}{\partial \zeta} = 0$
C	Tight $y_{\max}$ Mild $u'_{\max}$ Mild $u_{\max}$	$\left[\zeta^{\dagger f} \le \zeta^{*g} \le \zeta^{gh}\right] \cap \left[\tau_c^{*f} \le \tau_c^{gf}\right] \cap \left[\tau_c^{\dagger} \ge \frac{\gamma_g}{g_r(\zeta^{\dagger})}\right]$	$(\zeta^{*g}, \tau_c^{*g})$	On $\tau_c = \frac{\gamma_g}{g_r(\zeta)}$	$\gamma_{\mathrm{g}} - g_r(\zeta)\tau_c = 0$ $\frac{\partial \Phi_r}{\partial \zeta} g_r - \tau_c \frac{\partial \Phi_r}{\partial \tau_c} \frac{\partial g_r}{\partial \zeta} = 0$
D	Tight $y_{\max}$ Tight $u'_{\max}$ Mild $u_{\max}$	$\left[(\zeta^{*h} \ge \zeta^{gh}) \cap (\tau_c^{\dagger} < \tau_c^{\dagger h})\right]$ or $\left[(\zeta^{*g} > \zeta^{gh}) \cap \left(\tau_c^{\dagger} \ge \frac{\gamma_g}{g_r(\zeta^{\dagger})}\right)\right]$	$\left(\zeta^{gh}, \tau_c^{gh}\right)$	On the vertex by $\tau_c = \frac{\gamma_g}{g_r(\zeta)}$ and $\gamma_h = h_r(\zeta, \tau_c)$	$\gamma_g - \tau_c g_r(\zeta) = 0$ $\gamma_{\mathrm{h}} - h_r(\zeta, \tau_c) = 0$
E	Mild $y_{\max}$ Mild $u'_{\max}$ Tight $u_{\max}$	$\left[\left(\zeta^{\dagger} < \zeta^{\dagger f}\right) \cap \left(\tau_c^{fh} \le \tau_c^{*f}\right)\right]$ or $\left[(\zeta^{gh} > \zeta^{*g}) \cap \left(\tau_c^{gf} \ge \tau_c^{*f} \ge \tau_c^{fh}\right)\right]$	$\left(\zeta^{*f}, \tau_c^{*f}\right)$	On $\gamma_f = f_r(\zeta, \tau_c)$	$\gamma_{\mathrm{f}} - f_r(\zeta, \tau_c) = 0$ $\frac{\partial f_r}{\partial \tau_c}\frac{\partial \Phi_r}{\partial \zeta} - \frac{\partial f_r}{\partial \zeta}\frac{\partial \Phi_r}{\partial \tau_c} = 0$
F	Tight $y_{\max}$ Mild $u'_{\max}$ Tight $u_{\max}$	$\left[\zeta^{\dagger f} > \zeta^{*g} > \zeta^{gh}\right] \cap \left[\tau_c^{*f} > \tau_c^{gf}\right]$	$\left(\zeta^{gf}, \tau_c^{gf}\right)$	On the vertex by $\gamma_f = f_r(\zeta, \tau_c)$ and $\tau_c = \frac{\gamma_g}{g_r(\zeta)}$	$\gamma_{\mathrm{f}} - f_r(\zeta, \tau_c) = 0$ $\gamma_{\mathrm{g}} - \tau_c g_r(\zeta) = 0$
G	Mild $y_{\max}$ Tight $u'_{\max}$ Tight $u_{\max}$	$\left[\left(\zeta^{\dagger} < \zeta^{\dagger f}\right) \cap \left(\tau_c^{*f} \le \tau_c^{fh}\right)\right]$ or $\left[\left(\zeta^{gh} \ge \zeta^{*h} \ge \zeta^{\dagger f}\right) \cap \left(\tau_c^{\dagger} < \tau_c^{\dagger h}\right)\right]$	$\left(\zeta^{fh}, \tau_c^{fh}\right)$	On the vertex by $\gamma_f = f_r(\zeta, \tau_c)$ and $\gamma_h = h_r(\zeta, \tau_c)$	$\gamma_{\mathrm{f}} - f(\zeta, \tau_c) = 0$ $\gamma_{\mathrm{h}} - h(\zeta, \tau_c) = 0$

Table 2. Global optima of the constrained optimal regulatory control problem.

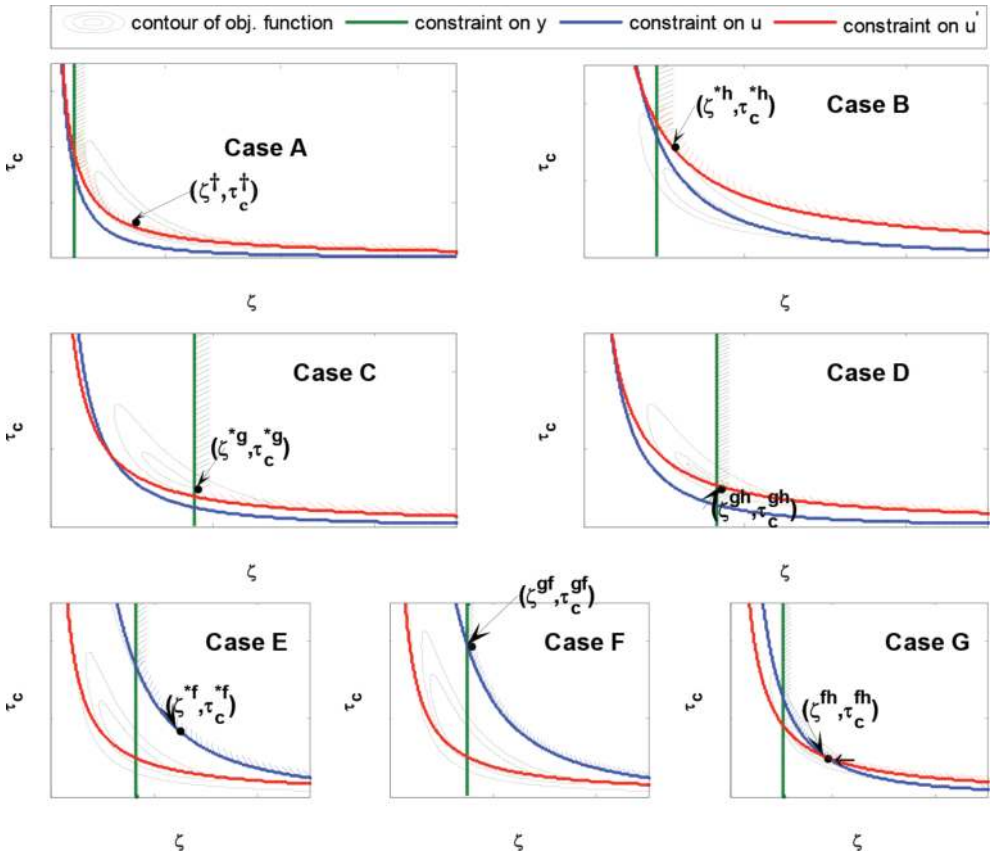

Figure 4. Contours, constraints, and possible locations of the global optimum in servo control case.

As indicated in **Figure 5**, the feasible region reduces in size as $u'_{\max}$ and $y_{\max}$decrease, exhibiting continued reduction until ceasing to exist if the constraints are lower than some minimum allowable values. Therefore, there exists a tangent point (ζ^t, τ_c^t) in (ζ, τ_c) space, where the two constraint curves of $u'_{\max}$ and $y_{\max}$ meet at a single point; this point equates to the smallest feasible $u'_{\max}$ for a given $y_{\max}$ (or the smallest feasible $y_{\max}$ for a given $u'_{\max}$) for different specifications of $u'_{\max}$ and $y_{\max}$.

Let $u'^t{}_{\max}$ be the smallest possible value of $u'_{\max}$. $u'^t{}_{\max}$ can be obtained when $\zeta = \zeta^t$. ζ^t can be calculated by solving the following equation:

$$\frac{dh_r(\zeta, \tau_c)}{d\zeta} = \frac{dh_r\left(\zeta, \gamma_g g_r^{-1}\right)}{d\zeta} = 0 \tag{17}$$

Case	Constraint specification	Condition	Global optimum	Location of global optimum	Calculation of global optimum
A	Mild y_{max} Mild u'_{max} Mild u_{max}	$\left[\zeta_{min} \le \zeta^{\dagger}\right] \cap \left[\tau_c^{\dagger} \ge \max\left(\tau_c^{*h}, \tau_c^{*f}\right)\right]$ where ζ_{min} is the minimum allowable damping factor by solving $g(\zeta_{min}) = \gamma_g$	$(\zeta^{\dagger}, \tau_c^{\dagger})$	In the interior of the feasible region	$\zeta^{\dagger} = \sqrt{\frac{1}{2}}$ $\tau_c^{\dagger} = \left(\frac{4\beta}{\alpha}\right)^{1/4}$
B	Mild y_{max} Tight u'_{max} Mild u_{max}	$\left[\zeta^{*h} > \max\left(\zeta^{hf}, \zeta_{min}\right)\right] \cap \left[\tau_c^{\dagger} < \max\left(\tau_c^{*h}, \tau_c^{*f}\right)\right]$	$(\zeta^{*h}, \tau_c^{*h})$	On $\tau_c^2 = \gamma_h^{-1} h_s(\zeta)$	$\zeta^{*h} = \left(\frac{4\beta\gamma_h^2}{\alpha} + \frac{1}{4}\right)^{1/2} \tau_c^{*h} = \left(\gamma_h^{-1} h_s\left(\zeta^{*h}\right)\right)^{\frac{1}{2}}$
C	Tight y_{max} Mild u'_{max} Mild u_{max}	$\left[\zeta_{min} > \zeta^{\dagger}\right] \cap \left[\tau_c^{*g} > \max\left(\tau_c^{gh}, \tau_c^{gf}\right)\right]$	$(\zeta^{*g}, \tau_c^{*g})$	On $g_s(\zeta) = \gamma_g$	$g_s(\zeta^{*g}) = \gamma_g$ $\tau_c^{*g} = \frac{1}{\zeta^{*g}} \left(\frac{3\beta}{\alpha\left(4(\zeta^{*g})^2 + 1\right)}\right)^{1/4}$
D	Tight y_{max} Tight u'_{max} Mild u_{max}	$\left[\tau_c^{\dagger} \ge \max\left(\tau_c^{*h}, \tau_c^{*f}\right) \cap \zeta_{min} > \zeta^{\dagger} \cap \tau_c^{gh} > \max\left(\tau_c^{*g}, \tau_c^{gf}\right)\right]$ or $\left[\tau_c^{\dagger} < \max\left(\tau_c^{*h}, \tau_c^{*f}\right) \cap \zeta^{gh} > \max\left(\zeta^{hf}, , \zeta^{*h}\right)\right]$	$\left(\zeta^{gh}, \tau_c^{gh}\right)$	On the vertex by $g_s(\zeta) = \gamma_g$ and $\tau_c^2 = \gamma_h^{-1} h_s(\zeta)$	$g_s\left(\zeta^{gh}\right) = \gamma_g$ $\tau_c^{gh} = \left(\gamma_h^{-1} h_s\left(\zeta^{gh}\right)\right)^{\frac{1}{2}}$
E	Mild y_{max} Mild u'_{max} Tight u_{max}	$\left[\tau_c^{\dagger} < \max\left(\tau_c^{*h}, \tau_c^{*f}\right)\right] \cap \left[\zeta_{min} < \zeta^{*f} < \zeta^{hf}\right]$	$\left(\zeta^{*f}, \tau_c^{*f}\right)$	On $f_s(\zeta, \tau_c) = \gamma_f$	$\gamma_f = f_s\left(\zeta^{*f}, \tau_c^{*f}\right)$ $\frac{\partial f_s(\zeta, \tau_c)}{\partial \tau_c} \frac{\partial \Phi_s}{\partial \zeta} - \frac{\partial f_s(\zeta, \tau_c)}{\partial \zeta} \frac{\partial \Phi_s}{\partial \tau_c} = 0$
F	Tight y_{max} Mild u'_{max} Tight u_{max}	$\left[\tau_c^{\dagger} \ge \max\left(\tau_c^{*h}, \tau_c^{*f}\right) \cap \left(\zeta_{min} > \zeta^{\dagger}\right) \cap \tau_c^{gf} > \max\left(\tau_c^{*g}, \tau_c^{gh}\right)\right]$ or $\left[\left(\tau_c^{\dagger} < \max(\tau_c^{*h}, \tau_c^{*f})\right) \cap \left(\zeta^{*f} < \zeta_{min} < \zeta^{hf}\right)\right]$	$\left(\zeta^{gf}, \tau_c^{gf}\right)$	On the vertex by $f_s(\zeta, \tau_c) = \gamma_f$ and $g_s(\zeta) = \gamma_g$	$g_s\left(\zeta^{gf}\right) = \gamma_g$ $\gamma_f = f_s\left(\zeta^{gf}, \tau_c^{gf}\right)$
G	Mild y_{max} Tight u'_{max} Tight u_{max}	$\left[\tau_c^{\dagger} < \max\left(\tau_c^{*h}, \tau_c^{*f}\right)\right] \cap \left[\zeta_{min} < \zeta^{*h} < \zeta^{hf}\right]$	$\left(\zeta^{fh}, \tau_c^{fh}\right)$	On the vertex by $f_s(\zeta, \tau_c) = \gamma_f$ and $\tau_c^2 = \gamma_h^{-1} h_s(\zeta)$	$\gamma_f = f_s\left(\zeta^{hf}, \tau_c^{hf}\right)$ $\tau_c^{hf} = \frac{1}{2\zeta^{hf}\sqrt{\gamma_h}}$

Table 3. Global optima of the constrained optimal servo control problem.

http://dx.doi.org/10.5772/intechopen.74301

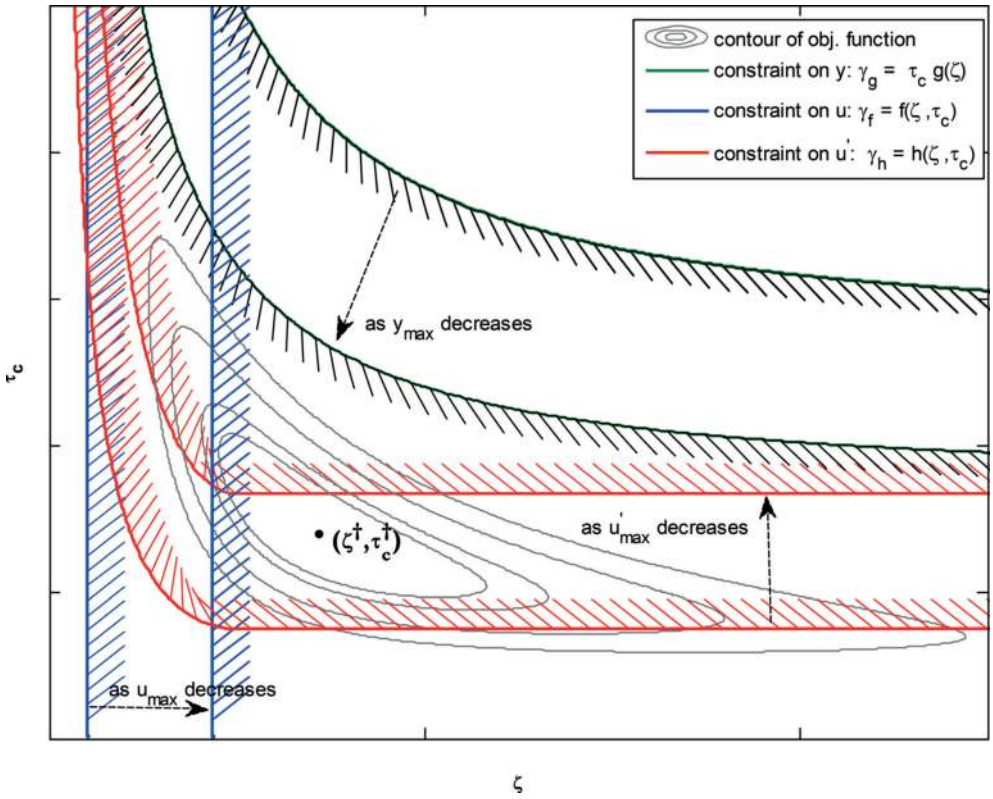

Figure 5. Effects of the constraint specifications y_{max}, u_{max}, and u'_{max} on the feasible region.

Once ζ^t is obtained, ${u'}^t_{max}$ can then be derived as follows:

$$ {u'}^t_{max} = h_r(\zeta^t)|\Delta D| \tag{18} $$

To sum up, if $u'_{max} \geq {u'}^t_{max}$, the constraint set (y_{max}, u'_{max}) is feasible; otherwise, it is infeasible.

Similarly, for a given u'_{max}, there is a minimum available y_{max} value below which the optimal control problem is not feasible. Let y^t_{max} be the smallest possible y_{max}. The values of y^t_{max} and ζ^t can be obtained by solving the following system of equations simultaneously:

$$ h_r\left(\zeta, \gamma_g g_r^{-1}\right) = \gamma_h \tag{19} $$

$$ \frac{dh_r\left(\zeta, \gamma_g g_r^{-1}\right)}{d\zeta} = 0 \tag{20} $$

To sum up, if $y_{max} \geq y^t_{max}$, then the constraint set (y_{max}, u'_{max}) is feasible; otherwise, it is infeasible.

Feasible $u_{\max}$ for a given feasible set $\left(y_{\max}, u'_{\max}\right)$: For a feasible $\left(y_{\max}, u'_{\max}\right)$, it can be intuitively inferred from the geometrical analysis of the constraint curves that any positive $u_{\max} \geq |\Delta D|$ will result in a feasible region if there is no intersection between the constraint curves of $\tau_c g_r(\zeta) = \gamma_g$ and $h_r(\zeta, \tau_c) = \gamma_h$. Furthermore, if the intersection, ζ^{gh}, exists, the constraint, $u_{\max}$, is feasible if $\zeta^{gh} \geq \zeta^{gf}$. To evaluate the existence of an intersection between the two constraint curves $\tau_c g_r(\zeta) = \gamma_g$ and $h_r(\zeta, \tau_c) = \gamma_h$, it is important to calculate $\tau_c(\infty)$, the value of τ_c where the two constraint curves are secant when $\zeta \to \infty$. $\tau_c(\infty)$ of each constraint curve can be obtained by solving the following equations:

$$\left[\tau_c(\infty) g_r(\zeta) = \gamma_g\right]_{\zeta \to \infty} \tag{21a}$$

$$\left[h_r(\zeta, \tau_c(\infty)) = \gamma_h\right]_{\zeta \to \infty} \tag{21b}$$

Because $\lim_{\zeta \to \infty} g_r(\zeta) = 1$ and $\lim_{\zeta \to \infty} h_r(\zeta, \tau_c) = 1/\tau_c = \gamma_h$, $\tau_c(\infty)$ of the two constraint curves are as follows:

$$\tau_c^g(\infty) = \gamma_g \tag{22a}$$

$$\tau_c^h(\infty) = \frac{1}{\gamma_h} \tag{22b}$$

A vertex ζ^{gh} exists when $\tau_c^g(\infty) \geq \tau_c^h(\infty)$. Therefore,

$$\gamma_g \geq \frac{1}{\gamma_h} \tag{23}$$

which yields

$$\left|\frac{y_{\max}}{K_p \Delta D}\right| \left|\frac{u'_{\max}}{\Delta D}\right| \geq 1 \tag{24}$$

Overall, for a given feasible $\left(y_{\max}, u'_{\max}\right)$, $u_{\max}$ is feasible under either of the following conditions: (1) Eq. (24) is not satisfied or (2) Eq. (24) is satisfied and $\zeta^{gh} \geq \zeta^{gf}$. Otherwise, $u_{\max}$ is not feasible and should be increased until one of the conditions is satisfied. Note that if $\left|\frac{y_{\max}}{K_p \Delta D}\right| \left|\frac{u'_{\max}}{\Delta D}\right| < 1$, no vertex point is formed by $\gamma_g = \tau_c g_r(\zeta)$ and $\gamma_h = h_r(\zeta, \tau_c)$, i.e., case D does not exist. In such a situation, for the purpose of evaluating the conditions presented in **Table 2**, any extremely large value can be assigned to ζ^{gh}.

Figure 6 illustrates a procedure applied to design a feasible constraint set $\left(y_{\max}, u'_{\max}, u_{\max}\right)$ and test its feasibility.

4.2. Optimal servo control

It is clear from their approaching values of $y(t), u(t), u'(t)$ as $t \to \infty$ that for the constraints by $y_{\max}$ and $u_{\max}$ to be feasible, they must be greater than $|\Delta Y_{sp}|$ and $|\Delta Y_{sp}/K|$, respectively, whereas the constraint by $u'_{\max}$ can be set to any nonnegative value. **Figure 7** illustrates how

http://dx.doi.org/10.5772/intechopen.74301

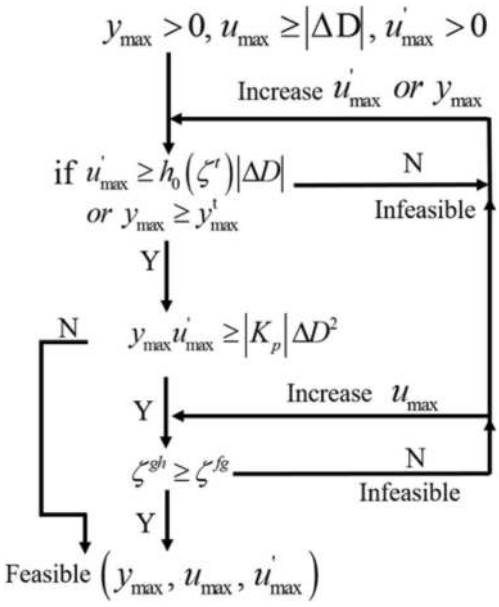

Figure 6. Procedure to design and test a feasible constraint set for optimal regulatory PI control of integrating system.

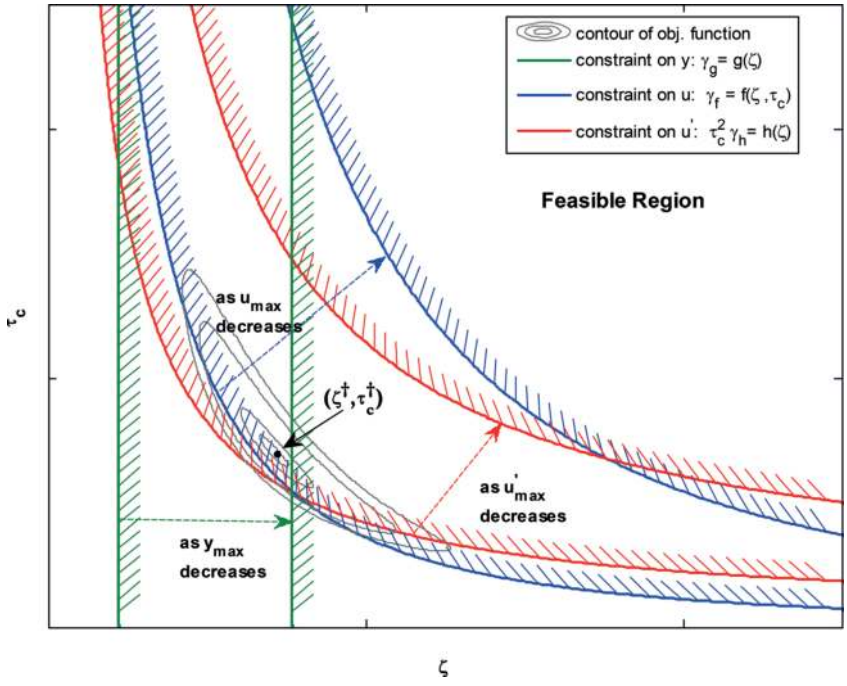

Figure 7. Effects of the constraint specifications y_{max}, u_{max}, and u'_{max} on the feasible region.

the three constraint specifications affect the feasible region. The constraint $\gamma_g \geq g_s(\zeta)$ vertically splits the region into two, while the constraints imposed by $\tau_c^2\gamma_h \geq h_s(\zeta)$ and $\gamma_f \geq f_s(\zeta, \tau_c)$ have a similar shape in (ζ, τ_c) space. It shows that for any feasible constraint set $(y_{max}, u'_{max}, u_{max})$, the feasible region is bounded below but unbounded in the upper side. This means that a decrease in y_{max}, u_{max} and u'_{max} will narrow down the feasible region delimited by the three constraints, but the feasible region will always exist. Moreover, the shape of the three constraints indicates the feasible region is always convex.

5. Closed-loop performance

5.1. Optimal regulatory control

Consider the following integrating process as

$$G_p(s) = \frac{1}{s} \tag{25}$$

Table 4 presents the examples of the seven possible aforementioned cases, as based on various constraint specifications. Simulations are carried out for weighting factors $\omega_y = \omega_{u'} = 0.5$.

Figure 8 presents the resulting process variable, $y(t)$, controller output, $u(t)$, and its rate of change, $u'(t)$, for the seven examples. As can be seen from the figure, the PI controller designed by the proposed method not only yields optimal control performance, but also strictly satisfies the respective y_{max}, u_{max}, and u'_{max} constraint requirements.

5.2. Optimal servo control

Consider the following integrating process

Example	Case	Constraint specification			PI parameter	
		y_{max}	u_{max}	u'_{max}	K_C	τ_I
1	A	0.70	2.70	2.70	1.41	1.41
2	B	0.70	2.70	1.11	1.10	1.10
3	C	0.36	2.70	2.70	1.93	1.51
4	D	0.285	2.70	2.10	2.10	0.69
5	E	0.70	1.105	2.70	1.96	2.95
6	F	0.30	1.20	2.70	2.18	0.98
7	G	0.70	1.20	1.37	1.37	1.56

Table 4. Constraint requirements and corresponding optimal PI parameters for regulatory control example.

http://dx.doi.org/10.5772/intechopen.74301

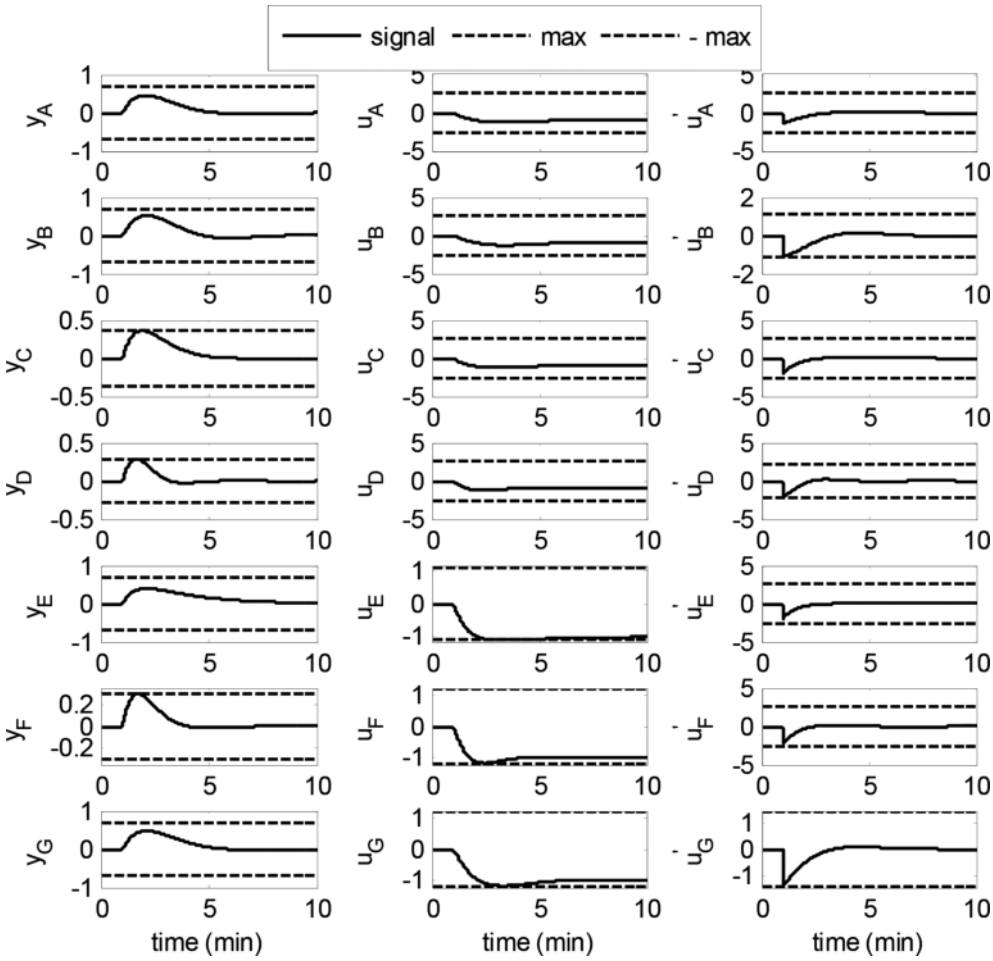

Figure 8. Time responses of the system for cases A to G: regulatory system.

$$G_p(s) = \frac{10}{s} \tag{26}$$

Table 5 lists the examples of the seven possible cases based on various constraint specifications. Simulations are carried out for weighting factors, $\omega_y = \omega_{u'} = 0.5$. **Figure 9** presents the time responses by the proposed optimal PI controller for the seven examples. As seen in the responses, the resulting optimal PI controllers not only provide the stable and optimal closed-loop responses, but also satisfy the y_{max}, u_{max}, and u'_{max} requirements, strictly.

Example	Case	Constraint specification			PI parameter	
		$y_{\max}$	$u_{\max}$	$u'_{\max}$	K_C	τ_I
1	A	1.2	0.5	1.5	1.41	1.414
2	B	1.2	0.5	0.5	0.79	1.58
3	C	1.03	0.5	1.5	1.52	1.46
4	D	1.03	0.5	1.03	1.51	1.47
5	E	1.2	0.3	1.5	1.53	2.42
6	F	1.03	0.41	1.5	1.38	1.61
7	G	1.2	0.4	1.17	2.15	1.83

Table 5. Constraint requirements and corresponding optimal PI parameters for servo control example.

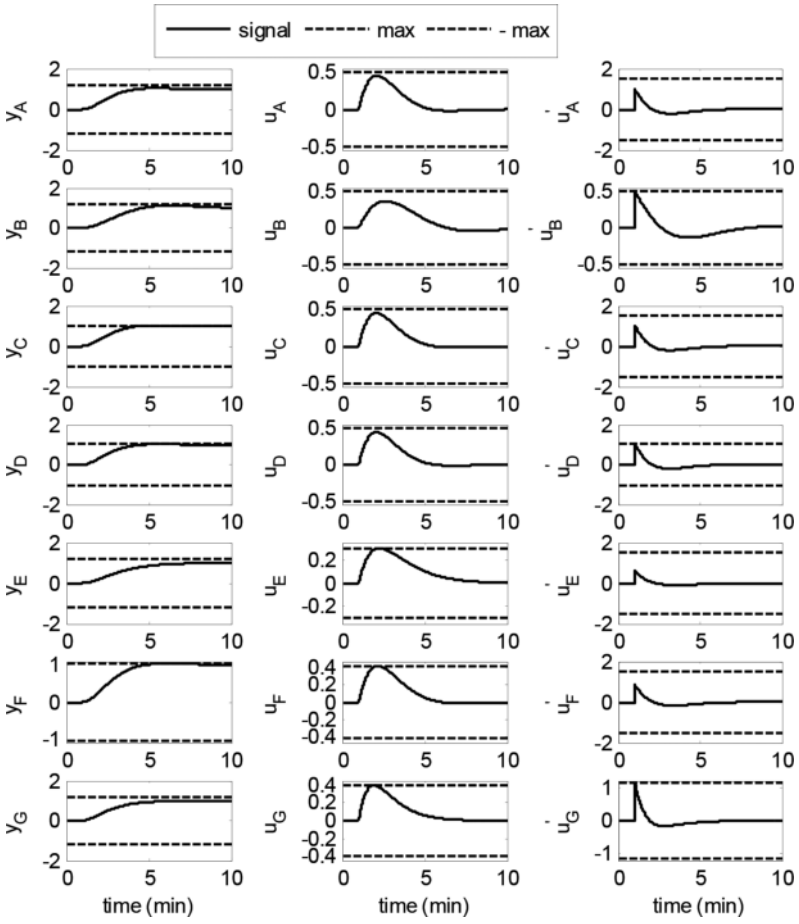

Figure 9. Time responses of the system for cases A to G: servo system.

6. Conclusions

A novel analytical design approach is introduced for optimal regulatory and servo PI control subjected to operational constraints and examined to integrating processes. Owing to incisive parameterization, a complex constrained optimal control problem can be reformulated and converted to a simple algebraic form in the new design parameter (ζ, τ_c) space, which allows finding the conditions and locations for the global optima by graphical analysis without having to rely on the numerical or black-box optimization effort. The proposed closed-form solution of the constrained optimal controller establishes a direct relationship between the control and plant parameters by which the optimal PI parameters can be obtained in an easy and quick manner. This approach also provides the following useful insights into how the control parameters affect the plant and how a feasible constraint set can be designed and checked in the constrained optimal control.

Acknowledgements

This research was supported by the Basic Science Research Program through the National Research Foundation of Korea (NRF) funded by the Ministry of Education (2015R1D1A3A01015621) and by the Priority Research Centers Program through the National Research Foundation of Korea (NRF) funded by the Ministry of Education (2014R1A6A1031189).

Conflict of interest

The authors confirm there are no conflicts of interest.

Author details

Rodrigue Tchamna and Moonyong Lee*

*Address all correspondence to: mynlee@yu.ac.kr

School of Chemical Engineering, Yeungnam University, Gyeongsan, Korea

References

[1] Lewis FL, Vrabie DL, Syrmos VL. Optimal Control. 3rd ed. New York: John Wiley and Sons; 2012. p. 553. DOI: 10.1002/9781118122631

[2] Siebenthal CD, Aris R. Studies in optimization—VII The application of Pontryagin's methods to the control of batch and tubular reactors. Chemical Engineering Science. 1964;**19**:747-761. DOI: 10.1016/0009-2509(64)85086-7

[3] Shin J, Lee J, Park S, Koo KK, Lee M. Analytical design of a proportional-integral controller for constrained optimal regulatory control of inventory loop. Control Engineering Practice. 2008;**16**:1391-1397. DOI: 10.1016/j.conengprac.2008.04.006

[4] Lee M, Shin J. Constrained optimal control of liquid level loop using a conventional proportional-integral controller. Chemical Engineering Communications. 2009;**196**:729-745. DOI: 10.1080/00986440802557393

[5] Lee M, Shin J, Lee J. Implement a constrained optimal control in a conventional level controller. Hydrocarbon Processing. 2010;**89**:71-76

[6] Lee M, Shin J, Lee J. Implement a constrained optimal control in a conventional level controller. Hydrocarbon Processing. 2010;**89**:81-85

[7] Nguyen VH, Yoshiyuki Y, Lee M. Optimization based approach for industrial PI controller design for optimal servo control of integrating process with constraints. Journal of Chemical Engineering of Japan. 2011;**44**:345-354. DOI: 10.1252/jcej.10we325

[8] Thu H, Lee M. Analytical design of proportional-integral controllers for the optimal control of first-order processes with operational constraints. Korean Journal of Chemical Engineering. 2013;**30**:2151-2162. DOI: 10.1007/s11814-013-0153-1

[9] Tchamna R, Lee M. Constraint handling optimal PI control of open-loop unstable process: Analytical approach. Korean Journal of Chemical Engineering. 2017;**34**:3067-3076. DOI: https://doi.org/10.1007/s1181

[10] Tchamna R, Lee M. Optimization approach for the analytical design of an industrial PI controller for the optimal regulatory control of first order processes under operational constraints. Journal of the Taiwan Institute of Chemical Engineers. 2017;**80**:85-99. DOI: 10.1016/j.jtice.2017.08.012

[11] Tchamna R, Lee M. Analytical design of an industrial two-term controller for optimal regulatory control of open-loop unstable processes under operational constraints. ISA Transactions. 2018;**72**:66-76. DOI: 10.1016/j.isatra.2017.11.002

[12] Vapnyarskii IB. Lagrange Multipliers. 1st ed. Heidelberg: Springer; 2001

[13] Boyd S, Vandenberghe L. Convex Optimization. 1st ed. Cambridge: Cambridge University Press; 2004. p. 727